Available online at www.sciencedirect.com
ScienceDirect
Journal of Sound and Vibration 300 (2007) 744–762
JOURNAL OF SOUND AND VIBRATION
www.elsevier.com/locate/jsvi

The measurement of the loss factors of beams and plates with constrained and unconstrained damping layers: A critical assessment

Denys J. Mead

Institute of Sound and Vibration Research, University of Southampton, Southampton SO17 1BJ, UK

Received 24 February 2006; received in revised form 22 August 2006; accepted 23 August 2006
Available online 17 October 2006

Abstract

Methods of measuring the loss factors of heavily damped beams and plates damped by uniform layers of visco-elastic damping are reviewed and compared. Deducing loss factors from measured spatial decay rates of free flexural waves in long beams is shown to be valid only for wave motion governed by the fourth-order flexural wave equation, so the method can only be used for unconstrained layer configurations. The usual approximation made in this method limits its accuracy and is examined. The flexural wave equation for three-layered sandwich beams and plates with constrained damping layers is of sixth order, so the spatial decay rate method is inapplicable for deducing loss factors. This is shown by both analysis and computer experiment. Reliable methods of damping measurement on finite damped sandwich beams are then investigated by computer experiment. Frequency-response functions for three-layered sandwich beams are computed for free–free and encastré beams, centrally excited. Loss factors of the fundamental symmetric modes are deduced from this computed response data as though it were experimental data. They are deduced by established methods such as the 'half-power-point' method, detailed analysis of Nyquist diagrams and the energy input method. Most of the deduced loss factors agree closely with the loss factors of the theoretical damped normal modes.

1. Introduction

Experimental measurement of the loss factors of heavily damped beams and plates became necessary in the early 1950s when the flexural vibration of plate and beam-like structures was first damped by the newly developed and efficient polymeric damping materials. The earliest materials were simply sprayed or trowelled on the structural surfaces in layers, the whole system then becoming the so-called 'unconstrained damping layer' configuration. More effective is the 'constrained layer' configuration in which the damping material is bonded and sandwiched between two plates or beams and constrained to undergo energy-dissipating shear strain.

The system damping had to be measured over as wide a frequency and temperature range as possible. A suitable method devised for unconstrained layer configurations involved a long and narrow damped beam,

E-mail address: djm@isvr.soton.uk.ac.

0022-460X/$ - see front matter © 2006 Elsevier Ltd. All rights reserved.
doi:10.1016/j.jsv.2006.08.023

Nomenclature

E_1, E_3	Young's moduli of the outer plates of the sandwich
EI	real part of the complex flexural stiffness
E_{total}	total maximum energy of vibration in one wavelength of a beam
EI_T	total flexural stiffness of the two outer plates of a sandwich
F	amplitude of harmonic force acting on a single-degree of freedom system
g	shear parameter
G	shear modulus of the damping layer
h_1, h_2, h_3	thickness of outer plate 1, damping layer (layer 2), outer plate 3
H	hysteretic damping coefficient of a single-degree of freedom system
k	complex wavenumber
k_r, k_i	real and imaginary parts of k
K	stiffness of a single-degree of freedom system
L	a prescribed standard length
m	mass per unit length
M	mass of a single-degree of freedom system
PE_λ	maximum potential energy stored in one wavelength of the beam
Q	the Q-factor, response amplitude at resonance/response at zero frequency
$T(\omega)$	complex transmissibility of vibration at frequency ω from the source to the receiver point
$w, w(x,t)$	(complex) transverse displacement of beam
X	the quotient $\text{Re}(w)/\text{Im}(w)$
Y	geometric parameter
β	loss factor of damping layer material
δ	exponential decay rate per wavelength
ε	phase difference between motions at two points
η	loss factor
λ	wavelength
ω	radian frequency
ω_n	natural frequency
Ω	non-dimensional frequency

excited harmonically at one end while the other end was made as non-reflective as possible. Well away from either end the predominant flexural wave motion in the beam was therefore that of a single flexural wave travelling away from the external forcing and decaying as it progressed. Its decay rate per wavelength was measured from which the flexural loss factor of the beam was deduced.

This method is quite legitimate for the unconstrained configuration. Oberst and Frankenfeld [1] had shown that when the two-layered configuration vibrates harmonically, its flexural rigidity could be regarded as being complex, its normalised imaginary part being the flexural loss factor, which is to be measured. Harmonic bending of such a beam is governed by the simple Euler–Bernoulli theory of bending (the 'EBT' theory) which leads to the familiar fourth-order differential equation for free flexural wave motion. The wavenumbers and decay rates of the wave motion for any given frequency are easily found from this and a simple relationship exists between the decay rate and the flexural loss factor. The loss factor is therefore easily found from the decay rate (and vice versa), so providing the legitimate basis for the 'long-beam method' of measuring the flexural loss factor of a beam with an unconstrained damping layer.

The same cannot be said of the constrained layer-damping configuration. Ross, Ungar and Kerwin [2,3] were the first to analyse this configuration and (like Oberst) sought its effective complex flexural stiffness. They found it as a function of the wavenumber and the properties of the cross-section which were contained in three important non-dimensional parameters. The wavenumber, of course, is a function of the flexural stiffness which, being a function of the wavenumber, suggests a vicious circle. They escaped it by assuming the spatial wave motion to be purely sinusoidal, i.e. to have no spatial decay. By specifying the wavelength of the motion (and hence the wavenumber) they found a corresponding flexural stiffness, loss factor and frequency of wave propagation.

Now spatially non-decaying sinusoidal motion can only exist if an external distributed harmonic loading acts on the system to prevent the inevitable spatial decay caused by energy dissipation in the damping layer. Such an 'external distributed loading' is an essential feature of the 'damped forced normal modes' introduced later on by DiTaranto, Mead and Markus [4,5]. The expression for the loss factor derived by Kerwin et al. is

quite correct within this context, but their use of the term 'effective flexural stiffness' has unfortunately misled some experimenters. They assumed it implied that the wave motion in a constrained layer configuration could be described by a fourth-order differential wave equation, as for the unconstrained layer beam. If that were true, the former relationship between the wave decay rate and the loss factor could be used to deduce loss factors from measured decay rates. Part of the purpose of this paper is to emphasise and demonstrate the error of this assumption and to compare some of the erroneous results it produces with the true values.

Wave motion in a three-layered constrained-layer damping configuration is actually governed by a sixth-order differential equation. First derived by Mead and Markus [6], it was then used by DiTaranto, Mead and Markus [4,5] to find the loss factors of finite sandwich beams and plates with arbitrary boundary conditions. Both their theory (the 'M&M' theory) and the sixth-order equation incorporate the same non-dimensional parameters as in Refs. [2,3], but an effective complex flexural modulus is no longer sought. A simple formula for the loss factor cannot be derived and the value of the loss factor can only be found by an iterative computational process.

The sixth-order equation and its solution will be used in this paper for three purposes:

(i) to find the complex wavenumbers of spatially decaying free harmonic waves in unbounded damped sandwich beams at any real frequency,
(ii) to find the complex frequencies and the true loss factors of the damped normal modes of finite sandwich beams with arbitrary boundary conditions,
(iii) to find the complex frequency response of finite damped sandwich beams with specific boundary conditions, excited by a single-point harmonic force.

From (i), it is easily shown that six spatially decaying flexural waves can exist at any real frequency, their wavenumbers occurring in three equal and opposite pairs. One of the pairs has a much smaller decay rate than the other two, so one of these waves necessarily dominates the motion in a constrained layered beam in the 'long beam' experiment already described. Its decay rate can be measured in the laboratory or can be computed at the desk. Part of the purpose of this paper is to investigate by 'computer experiment' whether these decay rates can be used to deduce the true loss factors of the beam.

From the complex frequencies[1] of (ii) the 'true loss factors ' may be found. The 'true loss factor' must be carefully defined and is best expressed in terms of an energy ratio to be quoted later (see also Ref. [7]). The M&M theory determines the complex frequencies of the complex 'damped normal modes' and identifies the normalised imaginary parts of these frequencies with the true loss factors. These have been shown to satisfy the energy definition of the loss factor although the M&M theory does not use this definition to compute them [8].

Now the damped normal modes of finite sandwich beams or plates cannot be purely excited in normal laboratory practice and they can only be excited in their purest form by their own unique distributions of external loading. These can never be simulated in practice. The usual (and simplest) practical form of excitation is by a single-point harmonic force of variable frequency. At a resonance forced in this way the response of the damped sandwich consists of a superposition of all the infinite number of damped normal modes (a well-known feature of even lightly damped structures) and it leads to problems of modal identification and loss factor measurement when resonance frequencies are closely spaced. However, well-established methods have been developed for analysing measured frequency-response functions to extract modal loss factors. Which of these methods, when used on heavily damped sandwich beams, yields similar (or identical) loss factors to the true loss factors needs to be ascertained, and is the other principal feature investigated in this paper by computer experiment. Exact frequency-response functions are computed for single-point excited sandwich beams with free–free or fully fixed (encastré) boundary conditions. Exact closed-form solutions of the sixth-order equation which satisfy the appropriate beam boundary conditions are used for this. The computed response functions are analysed to yield 'pseudo-experimental' loss factors to be compared with both the true computed loss factors of the damped normal modes and those deduced from decay rates in long beams, as predicted by computer experiment.

[1]The complex frequency concept must not be taken to imply any time-decay of the motion. The imaginary part actually represents the externally applied distributed loading required to maintain harmonic time-undecaying motion at a resonance frequency.

Mention must be made at this point of an excellent experimental and theoretical investigation undertaken by Lu and Douglas [9]. Basing their work on the sixth-order wave equation and carefully using the correct frequency-dependent material properties of the damping layer, they computed the frequency-response function of a freely supported damped sandwich beam over a frequency range extending beyond the fourth resonance. The experimental frequency-response function agreed excellently with the calculations, but no investigation was made into modal loss factors.

2. Spatial decay rates of free propagating wave motion in damped beams

2.1. Beams with unconstrained layers of damping material

When the damping material has linear elastic-hysteretic properties, the mode of harmonic flexural displacement of the beam $w(x)$ is governed by the fourth-order equation

$$EI(1+\mathrm{i}\eta)w'''' - m\omega^2 w = 0. \tag{1}$$

w'''' implies the fourth x-wise derivative of w. $EI(1+\mathrm{i}\eta)$ is the complex flexural stiffness of the whole section of the layered beam, m is the total mass per unit length of the beam and ω is the (radian) frequency. The complex stiffness is given by the expression first derived by Oberst and Frankenfeld [1] and involves the thicknesses and material properties of the two-layered beam. Further details of this and of other ways of deriving it are described elsewhere [10].

With the wave displacement expressed in the form $w(x) = A\exp(kx)\mathrm{e}^{\mathrm{i}\omega t}$, Eq. (1) yields four complex values for k given by $(m\omega^2/(EI(1+\mathrm{i}\eta)))^{1/4}$. Two of these represent wave motion decaying from left to right, while the other two decay from right to left. When a long damped beam is excited at its left-hand end, the first two of these are generated at that end but, as one of them decays much more rapidly than the other, its amplitude is negligible remote from the excited end. The other two waves are generated by reflections from any discontinuities or boundary to the right of the source, but if they are far enough away from the source or if the boundary is non-reflective, their magnitudes and presence can also be neglected. In the intermediate region of the beam the only significant motion is then that of a single wave decaying from left to right. Denote its complex wavenumber by $k_r + \mathrm{i}k_i$ so that

$$k_r + \mathrm{i}k_i = \left(\frac{m\omega^2}{EI(1+\mathrm{i}\eta)}\right)^{1/4}. \tag{2}$$

Of the four possible values of this, the wave with the lowest decay rate has the (k_r, k_i) values

$$k_i = \left(\frac{m\omega^2}{EI(1-\eta^2)}\right)^{1/4} \mathrm{Re}(1-\mathrm{i}\eta)^{1/4} \quad \text{and} \quad k_r = \left(\frac{m\omega^2}{EI(1-\eta^2)}\right)^{1/4} \mathrm{Im}(1-\mathrm{i}\eta)^{1/4}, \tag{3a,b}$$

k_i here is the usual 'wavenumber' which is numerically equal to $2\pi/\lambda$, λ being the wavelength of the motion which is relatively easy to measure on a vibrating beam. k_i should also be regarded as the phase difference between the motion of the beam at two locations along the beam separated by unit distance. The phase difference ε between two points separated by a distance x can be measured, so the wavenumber is ε/x and the wavelength is $\lambda = 2\pi x/\varepsilon$.

Now k_r is the exponential decay rate *per unit length* along the beam. The more easily measured quantity is the decay rate *per wavelength* , i.e. $k_r\lambda$. Denote this by δ, so

$$\delta = k_r\lambda = \frac{k_r}{k_i}2\pi. \tag{4}$$

To deduce EI and η from experimentally measured values of k_i and δ, one proceeds as follows. Rationalising Eq. (2) one obtains

$$EI(1+\mathrm{i}\eta) = \frac{m\omega^2}{(k_r+\mathrm{i}k_i)^4} = m\omega^2\left[\frac{(k_r-\mathrm{i}k_i)^4}{(k_r^2+k_i^2)^4}\right],$$

so

$$EI = \frac{m\omega^2}{(k_r^2 + k_i^2)^4}\,\mathrm{Re}(k_r + \mathrm{i}k_i)^4 \quad \text{and} \quad EI\eta = \frac{m\omega^2}{(k_r + \mathrm{i}k_i)^4}\,\mathrm{Im}(k_r + \mathrm{i}k_i)^4.$$

Expanding the bracketed functions of k_r and k_i and substituting $\delta/2\pi$ for k_r/k_i and $2\pi/\lambda$ for k_i one obtains

$$EI = m\omega^2\lambda^4\left[\frac{(\delta^4 - 24\delta^2\pi^2 + 16\pi^4)}{(\delta^4 - 4\pi^2)^4}\right] \tag{5}$$

and

$$\eta = \frac{8\pi\delta(4\pi^2 - \delta^2)}{(\delta^4 - 24\delta^2\pi^2 + 16\pi^4)} \tag{6}$$

If δ is small $\left(\delta^2 \ll (2\pi)^2\right)$ this becomes

$$\eta \approx 2\delta/\pi, \tag{7}$$

which is the approximate expression usually used. It can also be expressed in the form $\eta = 4k_r/k_i$.

Using the exact Eq. (6) one can examine the range of η over which this approximation is valid and Fig. 1 compares the exact and approximate values for values of η up to 1.0. The approximate values are evidently within 1% of the exact values if $\eta < 0.35$, within 7% if $\eta < 0.5$ and within 20% if $\eta < 1.0$. However, η values even as high as 0.2 are seldom realised in usable unconstrained-layer configurations, and spatial decay rates and wavelengths cannot easily be measured to commensurable degrees of accuracy.

2.2. Beams with constrained layers of damping material

This section considers the three-layer damping configuration in which the damping layer (the 'core') is sandwiched between two elastic layers ('face-plates'). The face-plates carry both bending stress and transverse shear stress but with negligible shear strain. Their elastic moduli (Young's modulus) are E_1 and E_3, respectively, and their thicknesses are h_1 and h_3. It will be assumed (as in Refs. [2–6]) that the core carries transverse shear stress and undergoes shear strain but has no significant longitudinal direct stress. Its complex shear modulus is $G(1 + \mathrm{i}\beta)$ and its thickness is h_2. It undergoes no transverse direct strain so all points on a transverse cross-section of the beam undergo the same transverse deflection w. Under these conditions the

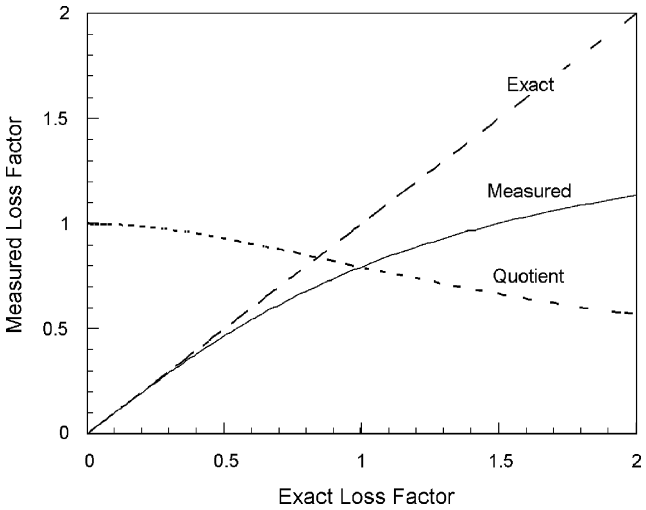

Fig. 1. Approximate loss factors deduced from the decay rates of flexural waves in a long damped Euler–Bernoulli beam and comparison with the exact values. (————) approximate values, (— — —) exact values, (– – – – –) quotient, i.e. approximate ÷ exact.

differential wave equation of harmonic motion w is found to be

$$EI_T\{w^{vi} - g(1+\mathrm{i}\beta)(1+Y)w^{iv}\} - \omega^2 m\{w'' - g(1+\mathrm{i}\beta)w\} = 0 \tag{8}$$

$EI_T = (E_1h_1^3E_3h_3^3)/12$ is the sum of the flexural stiffnesses of the face-plates acting independently. g is a 'shear parameter' proportional to G and defined in the Appendix. Y (also defined in the Appendix) is a geometric-cum-flexural stiffness parameter, which depends only upon the face-plate thicknesses and moduli and the core thickness.

Introduce the non-dimensional frequency Ω defined by

$$\Omega^2 = \omega^2 mL^4/EI_T, \tag{9}$$

where L is a length to be prescribed later. Set $w(x) = Ae^{kx}$ so that Eq. (8) yields the following sixth-order (bi-cubic) polynomial equation for k:

$$(kL)^6 - g(1+\mathrm{i}\beta)(1+Y)(kL)^4 - \Omega^2(kL)^2 + \Omega^2 g(1+\mathrm{i}\beta) = 0. \tag{10}$$

This has three pairs of complex roots, each of which corresponds to a flexural travelling wave which decays as it progresses. One of the pair with the lowest decay rates dominates the motion at locations in a long beam remote from a single-point harmonic exciting force and from a boundary. In principle, if the wavelength and decay rate could be measured, Eq. (10) could be used to deduce the core shear modulus G and loss factor β but this is found to be an exceedingly ill-conditioned and impracticable process. In any case, there are much better ways of measuring the material properties. Notice that Eq. (10) as it stands gives no indication of the loss factor of the whole beam, whatever that may mean.

It is instructive, however, firstly to consider how the three pairs of k vary with frequency and shear parameter. Once again, the k's have the complex form $k = k_r + \mathrm{i}k_i$ and Figs. 2a–c show how their real and imaginary parts (the decay index and wavenumber, respectively) and their moduli vary with frequency for a

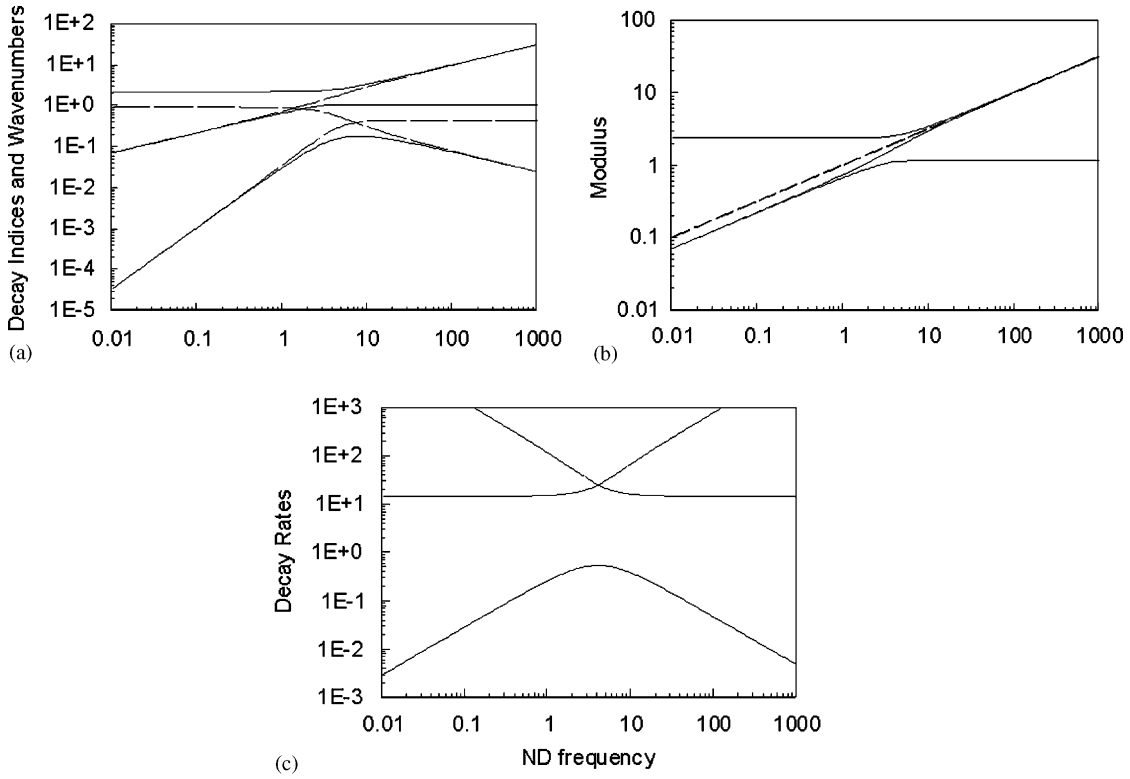

Fig. 2. The complex wave numbers of free wave motion in a damped three-layered sandwich beam: (a) real and imaginary parts, (b) the moduli, (c) decay rates per wavelength. $g = 1$, $Y = 3.162$, $\beta = 1$; in (a) —— decay indices (the real parts); in (b) ——— $\Omega^{1/2}$.

sandwich configuration with $g=1,\ Y=3.162\ (=\sqrt{10}),\ \beta=1$, values which correspond to a very soft, thin and highly damped sandwiched layer. Each of the three sets of k's varies with Ω in a distinctly different way, unlike those of the k's for the damped Euler beam which always vary in proportion to $\sqrt{\Omega}$. However, two of the sandwich sets are almost proportional to $\sqrt{\Omega}$ when $\Omega>40$. This is seen on Fig. 2b, which shows the moduli of each set and compares them with $\sqrt{\Omega}$.

Now the two sets which approach $\sqrt{\Omega}$ are those with the highest decay rates. The set of greatest interest is the one, which might be detected and measured in a 'long beam' experiment, i.e. the one with the lowest decay rate. Its decay rate reaches a maximum at a frequency of approximately 10, demonstrating the well-known feature of constrained layer damping that their damping properties reach peak values at specific frequencies governed by the values of g, Y and β.

The decay indices of Fig. 2a are the decay rates per unit length. The decay rates per wavelength of each wave motion ($\delta=(k_r/k_i)2\pi$, Eq. (4)) are shown in Fig. 2c. The lowest curve indicates even more clearly the characteristic variation of the damping with frequency. Such a curve as this might be generated from experimentally measured values, provided the motion is large enough to be measured accurately. It still remains, however, to deduce loss factors from such values. The formula relating loss factors to decay rates of damped Euler beams (Eq. (6)), being derived from the fourth-order wave equation, may be completely inapplicable to the sandwich beam, so the following alternative method will be investigated.

As already stated, the system loss factor can be defined in terms of an energy ratio as follows [7,8]:

$$\text{Loss factor, } \eta=\frac{1}{2\pi}\frac{\text{Total energy dissipated in the system per harmonic cycle}}{\text{maximum potential energy stored during the cycle}}. \tag{11}$$

It must be recognised that the maximum energy stored in different elements and locations in the damped system occurs, in general, at different times in the course of the cycle [8]. For example, the maximum energy in the core of the damped sandwich does not occur at the same time as the maximum energy in a face-plate and this must be taken into account when estimating the total maximum energy. Practical difficulties, however, preclude the use of this expression as a basis for the experimental determination of η. Instead one must depend upon the approximate equality of the maximum potential and maximum kinetic energies of the wave motion when the damping is small. They are exactly equal in each elemental length of both Euler and sandwich beams in the absence of damping but they become increasingly unequal as the damping increases in sandwich beams. This will be seen to limit the usefulness of the method.

Denote the total maximum energy (kinetic + potential) in one wavelength of the beam by E_{total}. This is proportional to the square of the displacement amplitude $|w(x')|^2$ at an arbitrary point x' within that wavelength, so $E_{\text{total}}=C|w(x')|^2$. ($C$ is simply the constant of proportionality). Over the next (adjacent) wavelength, the displacement amplitude at the corresponding point is reduced to $|w(x)|e^{-k_r\lambda}=|w(x)|e^{-\delta}$ so the total maximum energy is reduced to $C|w(x)|^2e^{-2\delta}$. The difference between these energies is $\delta E_\lambda=|w(x)|^2C(1-e^{-2\delta})$ which is the energy dissipated by the damping mechanism as the wave advances over the spatial cycle of one wavelength.[2] On the assumption that the total maximum potential energy is one-half of the total maximum energy, the maximum potential energy PE_λ in the first wavelength is $C|w(x')|^2/2$. Now substitute these expressions for PE_λ and δE_λ into the energy Eq. (11) for the loss factor to yield

$$\eta=\frac{1}{2\pi}\frac{\delta E_\lambda}{\text{PE}_\lambda}=\frac{(1-e^{-2\delta})}{\pi}. \tag{12}$$

The simple first-order approximation for $e^{-2\delta}$ in this leads to $\eta_{\text{approx}}=2\delta/\pi$ when δ is small, which is the same as given by Eq. (11).

Clearly, if δ becomes very large, η as given by the Eq. (12) approaches the obviously false value of $1/\pi$. The error stems from the actual inequality of the maximum kinetic and potential energies in a damped wave, especially when the decay rates are large. This feature applies particularly to the two waves of Fig. 2 with the higher decay rates and δ's. These are actually damped evanescent waves. It is well known that, even in the absence of damping, the potential and kinetic energies in evanescent waves are unequal. The difference between their maxima is balanced by reactive power from the source of excitation.

[2]It is the spatial equivalent of the energy dissipated in a temporal harmonic cycle as required in the energy definition of the loss factor.

It must be emphasised that the loss factors deduced in this way pertain to damped waves propagating freely away from a harmonic point-source. They do not necessarily apply to the constituent waves of resonating finite sandwich beams, a feature which will be explained and demonstrated later in this paper.

3. The loss factors of single-span simply supported sandwich beams

Ross, Ungar and Kerwin [2,3] assumed the transverse beam displacement varied with x and t in the simple sinusoidal form $w(x,t) = w_0 e^{i k_i x}$, i.e. with no spatial or temporal decay. This can only be achieved if some form of external distributed forcing acts on the beam, otherwise the wave must inevitably decay as it propagates. This external forcing characterises the 'damped normal modes' of DiTaranto, Mead and Markus [4,5], which will be considered in the next section. For the time being, it can be stated that the damped normal mode of a simply supported damped sandwich beam actually has the simple sinusoidal form given by the above expression, with k_i having a discrete value $2\pi n/L$ ($n = 1, 2, 3, \ldots$, etc. L is the beam length). Substituting this into Eq. (10) it yields, after rearrangement

$$\Omega^2 = \frac{(k_i L)^6 - g(1 + i\beta)(1 + Y)(k_i L)^4}{(k_i L)^2 + g(1 + i\beta)}. \tag{13}$$

The presence of the complex term $(1 + i\beta)$ on the right-hand side means that Ω^2 is complex and can be expressed in the form $\Omega^2(1 + i\eta)$. The imaginary part of this is directly related to the distributed forcing of the mode [4,5] and η has also been shown [8] to be the genuine loss factor of the damped forced mode as it satisfies the energy Eq. (11). The distributed forcing is of a particular kind, being equal to η times the inertia loading on the beam (i.e. to $\eta\omega^2 m w(x)$ per unit length) but is in phase with the local velocity. It provides a continuous input of energy into the beam, counteracting the energy loss due to the damping and maintaining the non-decaying modal motion.

The question arises as to whether the measured decay rates on the spatially decaying wave of a long, point-excited beam can yield the same loss factors as those a finite beam resonating in the supposedly spatial-sinusoidal waves of Ross, Ungar and Kerwin, or in the more complex damped normal modes of Mead & Markus (M&M). The question is addressed in this section.

The supposed advantage of obtaining loss factors from long-beam spatial decay rate measurements is the ability to find them at any frequency over a wide range. If there are no reflected waves in the forced motion, waves of any wavelength can be excited This contrasts with loss factor measurements of the modes of finite beams which can only be readily obtained at, or close to the widely spaced discrete resonant frequencies. But this is no problem when one conducts 'computer experiments' based on Eq. (13). Continuously changing L in Eq. (13) leads to a continuous change in the RUK frequency $\mathrm{Re}(\Omega)$, the associated modal loss factor η varying continuously with it. For each value of $\mathrm{Re}(\Omega)$, spatial decay rates of the long-beam, point-excited wave can be computed from Eqs. (11) or (12) and 'experimental loss factors' can be computed.

Some results obtained from this procedure are presented in Figs. 3a,b. These compare the loss factors of the simply supported beam vibrating in its fundamental damped normal mode with loss factors deduced from wave decay rates at the same frequencies. Two specific sets of Y's and β's are considered as indicated, with g and β being assumed to remain constant as Ω varies.[3] There is general similarity of form between the pairs of curves, each one of a pair reaching its maximum value at almost the same frequency. Over the almost straight 'skirts' of the curves, the modal values are approximately twice those obtained from decay rates. This is true for a wide range of g's, Y's and β's, including the low Y values which correspond to thin damping tapes on thick plates.

Now the frequency ranges of greatest practical interest are those in which loss factors pass through maximum values, as these are the ranges in which the high damping capacity of sandwich beam or plate configurations are best exploited. In these ranges the differences between the loss factors of the finite beam and those deduced from decay rates are most apparent. It has been found from further calculations that if $Y > 2.48$, the peak values from decay rates are greater than modal values, but are less if $Y < 2.48$. As Y

[3]The unreality of this for real damping materials is well known, but the assumption is justified in the present case since the only purpose is to compare the loss factors found by different methods in systems with identical parameters.

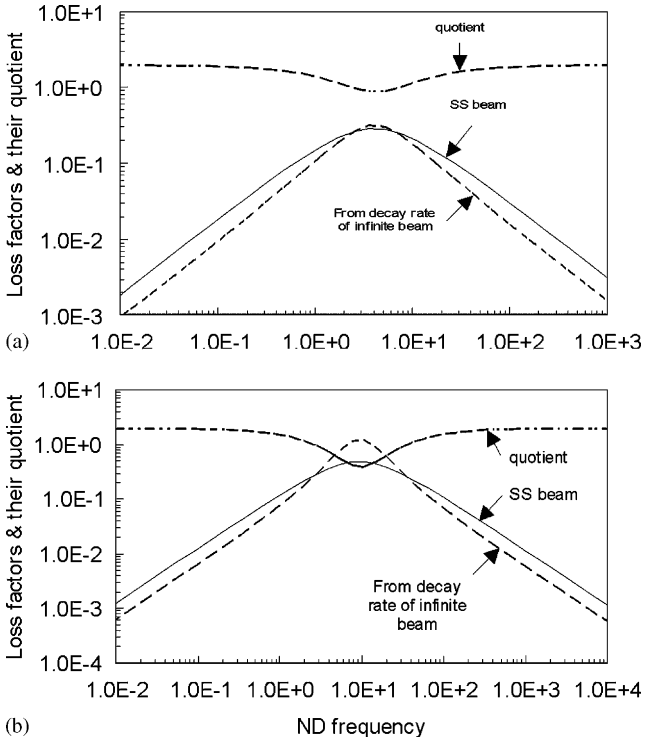

Fig. 3. (a,b) The loss factors of a finite simply supported beam vibrating in its fundamental damped normal mode compared with loss factors deduced from wave decay rates in a long beam.

increases beyond 2.48, these differences increase, and when $Y = 100$ (a very large value) the decay rate loss factor is about 10 times the modal value.

These results demonstrate that substantial disagreement exists between spatial decay rate loss factors and those of the damped normal modes of simply supported beams. The underlying reason is the critical dependence of the loss factor on both the nature and value of the wavenumber of the wave motion. In the decay rate 'experiment' the motion has a complex wavenumber whereas that of the simply supported beam is purely imaginary (i.e. a spatially sinusoidal motion). If the beam has other boundary conditions, its damped normal modes consist of waves with wavenumbers different from either of these. It remains to be seen whether any of these loss factors agree with loss factors which can be deduced from forced vibration experiments on finite beams. This will be investigated in the next section through further computer experiments.

4. The loss factors of single-span free–free and encastré sandwich beams

4.1. The general approach

The difficulty of manufacturing real simple supports for a sandwich beam specimen makes experiments on such beams impracticable but perfectly free or fully fixed (encastré) boundary conditions are relatively easy to simulate. Accordingly, this section computes the harmonic forced responses of free–free and encastré beams and analyses them as though they were experimentally measured data. In this way, 'pseudo-experimental' loss factors are determined by some well-known methods and are compared with values obtained from the M&M damped normal mode theory and the long-beam decay rate method. The responses are computed for beams with assigned ranges of g, Y and β and over frequency ranges around the fundamental resonances. The next sections outline the damped normal mode theory for sandwich beams and the theory for their forced vibration response. The methods used to deduce loss factors from computed responses are also described.

4.2. Outline of the damped normal mode and forced response theories

Damped normal modes consist of complex wave pairs, each with a wavenumber given by Eq. (10). Their transverse displacements in an infinite beam are best expressed in the exponential form $w(x) = A\exp(kx)$ but the hyperbolic form $A_S\sinh(kx) + A_C\cosh(kx)$ is more convenient for finite beams vibrating in damped normal modes. When the beam is supported symmetrically and the origin for x is taken midway between the supports, its symmetric modes are given by the sum of the even functions $\sum_{n=1}^{3} A_{Cn}\cosh(k_n x)$ and the symmetric modes by the sum of the odd functions $\sum_{n=1}^{3} A_{Sn}\sinh(k_n x)$. The total motion in each case must satisfy the boundary conditions of the beams and this, of course, can only be achieved at discrete resonant frequencies. For an undamped beam, these are the simple real natural frequencies, but when the beam is damped they are complex. When their squares are expressed in the form $\Omega^2(1+\mathrm{i}\eta)$ as already described, η is the loss factor of the damped normal mode and Ω is the resonance frequency.

Ω and η can only be computed by an iterative process which finds the $\Omega^2(1+\mathrm{i}\eta)$ roots of a complex characteristic determinant derived from the boundary conditions at the ends of the beam. Its terms are functions of both Ω^2 and the complex k's which themselves are functions of Ω^2. If the uniform beam is symmetrically supported and the appropriate hyperbolic functions of $k_n x$ are used for $w(x)$, satisfaction of the boundary condition at one end of the beam automatically satisfies them at the other. Details relating to the determinants for free–free and encastré sandwich beams are included in the Appendix which also sets up the equations for the responses of these beams to single-point harmonic forces. A closed form solution has been used for this as distinct from a series form of damped normal modes.

In the current exercise, the single exciting force is placed at the centre of the beam and the total generated motion is split into two parts:

(a) the motion generated by the force as though it were acting on an infinite beam extending indefinitely in both directions on either side of the force and
(b) the 'reverberant' motion in the finite beam generated by reflection of these waves from the actual boundaries.

To the right of the force, (a) is expressed in the exponential form $w_+(x) = \sum_{n=1}^{3} A_{\infty,n}\mathrm{e}^{-k_n x}$, the motion to the left having similar form. The A's for the right and left-hand wave-sets are found by satisfying the continuity and equilibrium conditions at the loading point, and from these A's one easily determines the total 'infinite beam' motion at any point x. In particular, they are found at the finite beam boundary locations.

The reverberant motion generated by boundary reflection is best described by the hyperbolic functions, i.e. by $\sum_{n=1}^{3} A_{Cn}\cosh(k_n x)$ for the symmetric modes. The A_{Cn}'s in this, of course, are different from those defining the damped normal modes. The total infinite-beam + reverberant motion must satisfy the boundary conditions at the ends of the beam, which lead to a set of three equations for the three unknown A_{Cn}'s. Solving for these, one then readily computes the total 'infinite beam' + reverberant wave motion for any point in the beam (see Ref. [11] for the first presentation of this method for sandwich beams and plates).

4.3. Methods of deriving loss factors from computed or measured responses

These will be described by reference to Fig. 4, which shows the variation with frequency of the real and imaginary parts of computed responses at the centre of a free–free sandwich beam excited by a central harmonic force of constant amplitude. The frequency range covered is only that around the fundamental resonance. The particular core properties used for this diagram were $g = 1$, $Y = 10$, $\beta = 1.0$ ($Y = 10$ represents a core which is slightly thinner than one of the (equal) face-plates; $\beta = 1$ and $g = 1$ are typical values for damped sandwich cores). The modulus of the imaginary part is plotted to allow its whole positive and negative range to be included on the logarithmic plot.

The real parts of the response are shown in two forms, 'uncorrected' and 'corrected', the uncorrected part increasing indefinitely as $\Omega \to 0$. This is associated with the rigid body translation of the beam which increases indefinitely because the rigid body *acceleration* amplitude remains constant as the forcing frequency changes. In the region of the fundamental resonance frequency the rigid body translation still contributes significantly

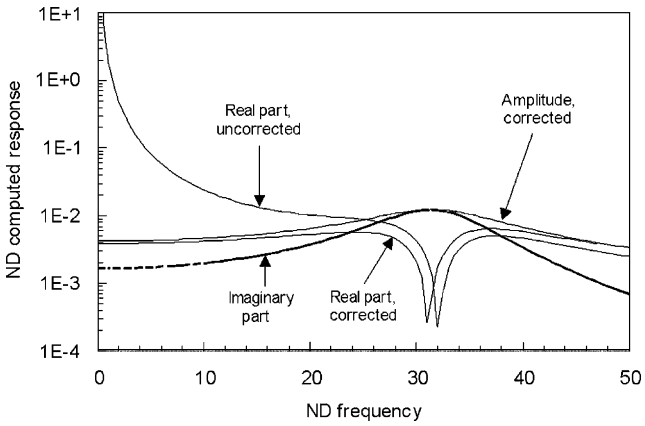

Fig. 4. The variation with frequency of the real and imaginary parts of the computed responses at the centre of a free–free sandwich beam excited by a central harmonic force of constant amplitude. $g = 1$, $Y = 10$, $\beta = 1.0$.

to the total response and distorts the modal response diagrams. These can only be found accurately by a two-stage correction process, the first of which is to remove the (real) rigid body component from the computed total. Now the rigid body displacement varies inversely with Ω^2 so its actual values near the resonance can easily be deduced from its values as $\Omega \to 0$. The required correction is easily carried out by computer subtraction but probably could not be done with sufficient accuracy on actual experimental data. The computed and corrected real part is also shown on Fig. 4 and now bears much closer resemblance to a conventional highly damped resonance response curve.

Modal properties such as the loss factor are frequently deduced from experimental response data plotted in the form of Nyquist diagrams on which the real and imaginary parts of the measured or computed modal response at different frequencies are plotted one against the another. It has long been known [12] that the Nyquist diagram for a single-degree-of-freedom system with hysteretic damping is a perfect circle centred on the imaginary axis and ending (as $\Omega \to \infty$) at the origin. Figs. 5a,b show the Nyquist diagrams for the uncorrected and first-stage corrected computed responses. Only part of the uncorrected diagram is at all circular. The first-stage correction makes it 'much more' circular but it is still not centred on the imaginary axis. This is due to the presence in the total response of the small and predominantly real contributions from all the higher modes of vibration which (at the fundamental frequency) are vibrating below their own resonances. Over the frequency range of primary interest around the circle, it can be assumed that the total higher-mode contribution remains constant, the value of which must be subtracted from the first-stage corrected values. It is found by a process of locating the centre of a true circle which best-fits a selected number of data points (a minimum of three) around the first-stage corrected diagram. From the coordinates of this centre one finds the constant to be subtracted from each data point of the first-stage corrected circle to move it to its 'correct sdof position', centred on the imaginary axis. Fig. 5c shows the result of this procedure on the first-stage corrected circle of Fig. 5b. The best-fit circle is not on this but on the computer screen was indistinguishable from the 'circle' shown.

It remains now to deduce the modal loss factor from the stage 2, fully corrected circle. Three methods can be employed:

(i) From a simple estimate of the Q-factor (the 'magnification factor').
(ii) From the half-power frequency bandwidth of the amplitude-response curve.
(iii) From the quotient of the real and imaginary parts of the response.
(iv) From the imaginary part at true resonance, used in an energy input method.

Method (i) utilises very little data from the corrected circle. It assumes that only one mode participates in the total motion after the rigid body component has been removed and it only requires the amplitudes of response at a very low frequency and at the resonance frequency. The quotient of these yields the loss factor if

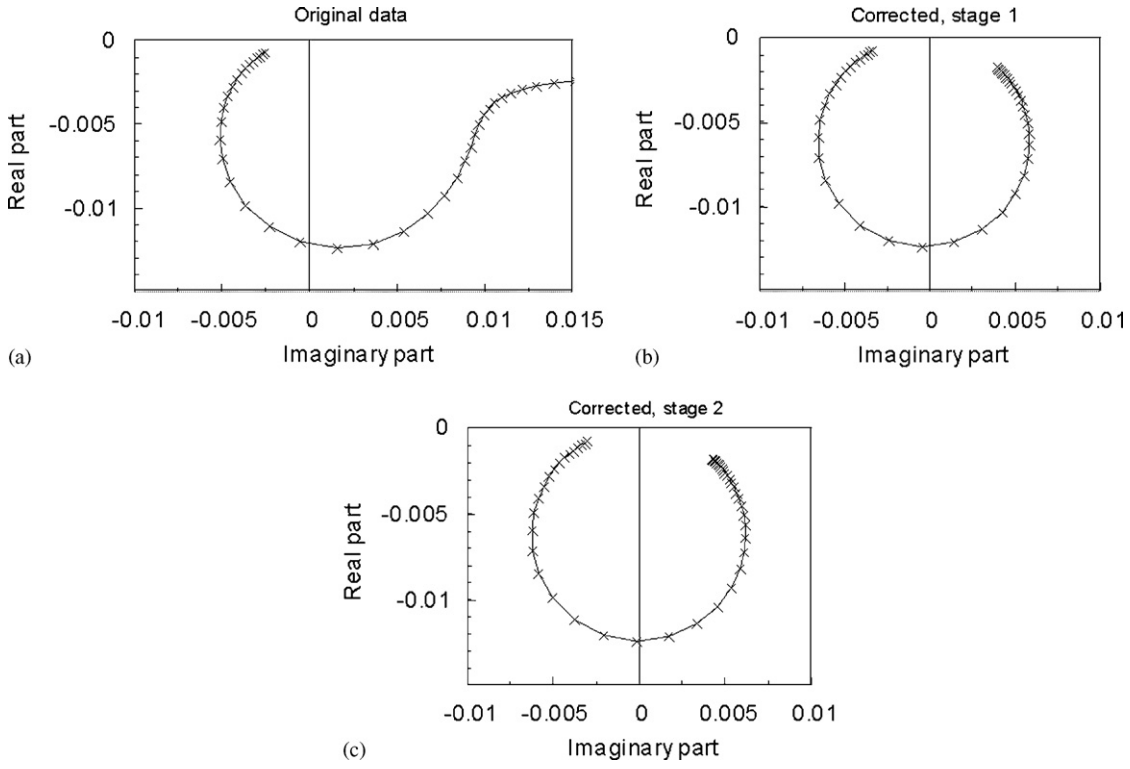

Fig. 5. Nyquist diagrams for the uncorrected response and the first- and second-stage corrected responses of Fig. 4.

the system truly has just one degree of freedom. The method can be used for a free–free beam in the current computer experiment since precise removal of the rigid body response component can be achieved, but is unlikely to be practicable in a laboratory experiment.

Method (ii) is too well known to require explanation or description. Method (iii) is based upon equations for the forced harmonic vibration of a simple hysteretically damped system with one degree of freedom, as follows.

The equation for the harmonic displacement of the system is $[-M\omega^2 + (K + \mathrm{i}H)]w = F$ or $\{[1 - (\omega/\omega_n)^2] + \mathrm{i}\eta\}w = F/K$. $\omega_n^2 = K/M$ and $\eta = H/K$ is the system loss factor. The real and imaginary parts of w are, respectively

$$\mathrm{Re}(w) = \frac{\left[1 - (\omega/\omega_n)^2\right]}{\left[1 - (\omega/\omega_n)\right]^2 + \eta^2} F/K \quad \text{and} \quad \mathrm{Im}(w) = \frac{-\eta}{\left[1 - (\omega/\omega_n)^2\right]^2 + \eta^2} F/K, \tag{14a,b}$$

so

$$\eta = -\frac{\mathrm{Im}(w)}{\mathrm{Re}(w)}\left[1 - (\omega/\omega_n)^2\right]. \tag{15}$$

It appears that Eq. (15) could be used to find the loss factor of the ideal system from values of $\mathrm{Re}(w)$ and $\mathrm{Im}(w)$ computed or measured at *any* frequency. In practice it runs into trouble when ω is very close to ω_n as the value when $\omega = \omega_n$ is indeterminate. At frequencies very close to ω_n the smallest errors in $\mathrm{Re}(w)$ or $\mathrm{Im}(w)$ lead to very inaccurate values of η, but these difficulties are circumvented by the following modified approach.

Rewrite Eq. (15) in the form $\eta[\mathrm{Re}(w)/\mathrm{Im}(w)] = -[1 - (\omega/\omega_n)^2]$. Differentiate both sides of this with respect to ω and rearrange to yield

$$\eta = \frac{2}{\omega_n^2} \frac{\omega}{\left((\mathrm{d}/\mathrm{d}\omega)\left(\mathrm{Re}(w)/\mathrm{Im}(w)\right)\right)}. \tag{16}$$

All the terms in this behave sensibly in the important frequency range close to ω_n. Approximate values of the derivative can be obtained at different frequencies from the discrete measured or computed values of Re(w) and Im(w). Denote by X_j, the quotient Re(w)/Im(w) at frequency ω_j, so its derivative in finite difference form is

$$\frac{\mathrm{d}X}{\mathrm{d}\omega} = \frac{(X_j - X_{j-1})}{(\omega_j - \omega_{j-1})}$$

and the corresponding value of η_j is

$$\eta_j \approx 2\frac{\omega_j}{\omega_n^2}\frac{(\omega_j - \omega_{j-1})}{(X_j - X_{j-1})}. \tag{17}$$

The degree of approximation in this depends, of course, on the size of the frequency interval $(\omega_j - \omega_{j-1})$ and on the accuracy of the available X_j's. Like Eq. (15), Eq. (17) is true for *any* value of ω_j provided the system really has just one degree of freedom. For a real multi-degree of freedom system, satisfactory values of $\boldsymbol{\eta}$ can usually be derived only from a restricted frequency range close to ω_n.

The value thus obtained for η depends on $\omega_n^2 = K/M$. ω_n can easily be identified from the fully corrected Nyquist diagram as the frequency at which the imaginary part of the response vector vanishes. This shows yet again the need for the two-stage correction of the measured or computed data.

Method (iv), based on the energy Eq. (11) for the loss factor, requires knowledge of both the energy dissipated (= the energy input into the system) and the maximum potential energy when the system vibrates in the required mode. In the laboratory, measurement of the energy input is a common experimental procedure, being obtained from the product of the amplitude of the exciting force and the imaginary part of the displacement response at the excitation point. The maximum potential energy is found most readily at the frequency at which the real part of the driving point response is zero, for then the maximum kinetic and potential energies are equal. The kinetic energy can be evaluated by length-wise integration of the product of the known mass distribution and the square of the measured vibration amplitude. However, this laboratory procedure was not used in the current computational experiment. The exact potential energy was evaluated from the exact computed modes of forced vibration but for conciseness the detailed procedure is not presented here.

As method (iv) involves integrated quantities over the whole length of the beam, the loss factors it yields are less dependent on the location of the response measuring point than those of methods (i), (ii) and (iii).

4.4. Systems subjected to prescribed harmonic motions; motion-excited beams

The previous section relates to systems excited by a variable-frequency *force* of constant amplitude. Now a free–free beam, centrally mounted on a relatively massive shaker, can be 'motion-excited' at a constant amplitude of *displacement* and the loss factor can be deduced from the measured (or computed) frequency-dependent transmissibility, $T(\omega)$. This is the ratio of the complex displacement at (say) the tip of the beam to the enforced central displacement, and at its fundamental resonance becomes the so-called 'Q-factor'. For the ideal single degree of freedom system, this is equal to $1/\eta$.

The resonances occur at the anti-resonance frequencies of the force-excited beam, the lowest of which is below the fundamental resonance of the force-excited beam. If both methods of excitation are used on the same beam, a loss factor can be obtained at an additional discrete frequency, but it must be recognised that it belongs to a different class of flexural mode. The force-excited modes are genuine 'free–free' flexural modes but the motion-excited modes are those of a cantilever of half the overall beam length, its modal displacements being superimposed upon a rigid body motion.

The transmissibility of the motion-excited beam is easily found from the same equations and the same computer programme as used for constant force excitation, after dividing the computed force-excited tip displacement by the computed source displacement. The loss factor can then be deduced from this by the Q-factor method (not recommended!) or preferably by analysing the Nyquist diagram of $T(\omega)$ by methods similar to those already described.

Table 1
Comparison of loss factors found by eleven different methods for a sandwich beam with $g = 1$, $Y = 10$, $\beta = 1.0$

Method	Free-free beam		Encastré beam	
	η	Ω_n	η	Ω_n
Forced response, from the Q-factor	0.373	31.2	0.19	24.96
Forced response, from 1/2 power bandwidth	0.41	31.2	0.188	24.96
Forced response, from component quotient	0.397	(20.0)[a]	0.186	(15.38)[a]
Forced response, from component derivatives	0.406	31.2	0.186	24.96
Forced response, from energy input	0.386	31.2	0.148	24.96
Damped normal mode theory (M&M)	**0.396**	**31.34**	**0.186**	**24.97**
From spatial decay rate method, Eq. (12)	0.192	31.34	0.215	24.97
From spatial decay rate method, Eq. (7)	0.294	31.34	0.357	24.97
Transmissibility, from the Q-factor	0.238	20.1	—	—
Transmissibility, from 1/2 power bandwidth	0.358	20.1	—	—
Transmissibility, from quotient derivative	0.351	20.1	—	—
Transmissibility, from energy input	0.365	21.1	—	—

[a]Arbitrary frequencies; the loss factors deduced at Ω_n were indeterminate.

4.5. Loss factors derived from computed responses

The four methods of Section 4.3 have been used to estimate the loss factors of the fundamental modes of free–free and encastré sandwich beams with $g = 1$, $Y = 10$, $\beta = 1.0$ (the same parameter values as considered for the free-free beam of Fig. 4). Loss factors of these modes have also been computed by the M&M theory. Values, which would be predicted by the two spatial decay rate methods, have been computed for the same frequencies as the resonance frequencies of the M&M damped normal modes. All these results are compared in Table 1. Good agreement is seen between most of the loss factors deduced from finite-beam forced vibration data and those from the damped normal mode theory.

Loss factors were found from transmissibility data by the same four methods as above but the theoretical loss factor for the corresponding damped normal mode was not determined. It required a larger computational programme than that for the damped normal modes of free–free or encastré beams and had not been developed[4]. The Q-factor method has previously been used in practice to find loss factors of motion-excited systems, use being made of the relationship $\eta = 1/T(\omega_n)$ in which ω_n is the frequency at which the real part of $T(\omega)$ vanishes. However, when this method is applied to motion-excited *continuous* systems, it suffers from the essential dependence of its η value on the point at which $T(\omega)$ is measured. The value quoted in Table 1 was derived from the transmissibility of the beam at its tip and is significantly different from the other three values which were also derived from the tip transmissibility and which all agree well amongst themselves. When derived from the transmissibility at a point about 1/6th of the beam length from the tip it is found to be almost equal to the value derived from the energy input which is quite independent of the measuring point. For quite different reasons, the loss factors deduced by all the other methods may be found to depend on the response location to a much smaller extent.

The agreement between the values deduced from the forced vibration responses and those of the M&M damped normal modes is significant. The damped normal modes are complex and are excited by a hypothetical distributed force distribution. They are not identical to the modes excited by single-point harmonic forces and although they may be similar, there is no a priori reason why the loss factors of the differing modes should be as close as they have been found to be. On the other hand, the loss factors deduced from free-wave spatial decay calculations or measurements are different from all the others by very significant

[4]As already stated, the mode of vibration at the transmissibility resonance is actually that of beam of half the total length, free at one end and 'clamped-sliding' at the other. Its mode is neither symmetric nor anti-symmetric and the six boundary conditions to be satisfied lead to a 6×6 complex determinantal frequency equation, instead of the 3×3 for symmetric modes.

Table 2
Comparison of loss factors found by three different methods for free-free damped sandwich beams with different combinations of g, Y and β

g	Y	β	Method	η	Ω_n
100	10	0.5	Damped normal mode theory (M&M)	0.0394	71.1
			Forced response, from quotient derivative	0.0394	71.08
			From spatial decay rate, Eq. (7)	0.0761	72.12
10	31.62	1	Damped normal mode theory (M&M)	0.347	95.64
			Forced response, from quotient derivative	0.35	95.4
			From spatial decay rate, Eq. (7)	0.709	95.64
1.78	0.5	1.5	Damped normal mode theory (M&M)	0.0819	23.41
			Forced response, from quotient derivative	0.0823	23.4
			From spatial decay rate, Eq. (7)	0.0485	23.41

amounts, sometimes being greater and sometimes less. The spatial decay rate method is therefore seen to be quite unsuitable for the measurement of modal loss factors of damped sandwich beams.

This conclusion is drawn from results corresponding to just one set of g, Y and β values. Table 2 suggests its generality by showing the loss factors for free–free sandwich beams with three different combinations of g, Y and β. In every case, the damped normal mode values agree closely with those deduced from finite-beam forced vibration data, but they differ widely from those deduced from spatial decay rates. Spatial decay rates yield a single loss factor for any given frequency, whereas finite sandwich beams which resonate at that frequency and have the same layer thicknesses and properties have loss factors which depend on the boundary conditions [4]. This further confirms the above conclusion.

5. Conclusions

Loss factors of damped sandwich beams cannot be reliably deduced from measured spatial decay rates of flexural waves in long beams and have been shown to differ substantially from the loss factors of resonating finite sandwich beams. They may be greater or less than the finite beam loss factors even when measured at the same frequencies.

Computer-experiments on finite beams forced harmonically close to resonance yield loss factors very close to those predicted by the Mead–Markus theory of complex damped normal modes. This has been confirmed for both free–free and encastré sandwich beams. The well-known methods of finding loss factors by the $\frac{1}{2}$-power bandwidth method and by measurement of the energy input at resonance have been shown to be accurate for even highly damped sandwich beams, and so also have methods which analyse the complex components of the forced response close to (and even remote from) resonance frequencies. In principle, these methods can be used to find loss factors from measured responses close to both resonances and anti-resonance frequencies, although responses actually measured near to anti-resonance frequencies may be insufficiently accurate for this purpose.

Sandwich beam loss factors depend not only on the frequency, but also on the mode of vibration. Beams (or plates) which are identical in all respects apart from their lengths and boundary conditions but which resonate at the same frequencies, have different loss factors. This difference is most pronounced in the fundamental modes.

Computer experiments on damped sandwich beams are capable of yielding loss factors of multi-figure accuracy. This, of course, is impossible from actual laboratory data. Real sandwich beams in the laboratory behave in a notoriously unpredictable manner. Unless extreme precautions are taken they can yield different loss factors at different times of day, apparently independently of ambient conditions! In spite of this, the experimenter should use the most reliable methods available to measure the loss factors. The results of this paper show those in which confidence may be placed.

Appendix A. Equations for the frequency response and loss factors of finite damped sandwich beams

Fig. A1 shows the dimensions and loads on the cross-section of a three-layer sandwich beam. The elastic (Young's) moduli of the face-plates are E_1 and E_3. The complex shear modulus of the core is $G(1+\mathrm{i}\beta)$. Its longitudinal elastic modulus is assumed to be negligible so $E_2 = 0$. The transverse direct strain in the core is assumed to be zero so the transverse (flexural) displacement $w(x,t)$ is the same across a given section. The differential equation governing the flexural wave motion in the sandwich when it vibrates freely at frequency ω is then

$$EI_T\{w^{vi} - g(1+\mathrm{i}\beta)(1+Y)w^{iv}\} - \omega^2 m\{w^{ii} - g(1+\mathrm{i}\beta)w\} = 0, \tag{A.1}$$

where $EI_T = \frac{1}{12}(E_1h_1^3 + E_3h_3^3)$ is the sum of the flexural rigidities of the two face-plates when each plate bends independently with the same $w(x)$.

g is a 'shear parameter' and Y the 'geometric parameter' defined by

$$g' = \frac{G}{h_2}\left\{\frac{1}{E_1h_1} + \frac{1}{E_3h_3}\right\}, \quad Y = \frac{d_{123}^2}{EI_T}\left(\frac{1}{E_1h_1} + \frac{1}{E_3h_3}\right)^{-1}. \tag{A.2a,b}$$

In physical terms Y can be defined by the relationship

$$(1+Y) = \frac{\text{Flextural stiffness of the whole beam section when } G=\infty}{EI_T}.$$

Define the non-dimensional frequency Ω by $\Omega^2 = \omega^2 mL^4/EI_T$ where L can be any arbitrary length but for a finite beam is most conveniently taken as the beam length. For an infinite beam it will be taken as unity.

Define also the non-dimensional shear parameter

$$g = \frac{GL^2}{h_2}\left\{\frac{1}{E_1h_1} + \frac{1}{E_3h_3}\right\}$$

and the non-dimensional wavenumbers $\lambda_n = k_nL$. With $L=1$ the kL's of Eq. (10) in the main text are automatically the wavenumbers per unit length.

Important relationships between the forces and moments acting on the section and the beam displacement w and its derivatives were first presented in Ref. [3] and are as follows.

The total vertical shear force on a beam section:

$$S = \frac{EI_T}{g(1+\mathrm{i}\beta)}\left[w^v + g(1+\mathrm{i}\beta)(1+Y)w''' + \Omega^2 w'\right]. \tag{A.3}$$

The resultant longitudinal force on a face-plate section (equal and opposite in each plate)

$$P = \frac{EI_T}{g(1+\mathrm{i}\beta)}\left(\frac{1}{d_{123}}\right)\left[w^{iv} + g(1+\mathrm{i}\beta)w'' + \Omega^2 w\right]. \tag{A.4}$$

The total bending moment acting on the beam section:

$$M = M_1 + M_3 + P_1\left(h_2 + \frac{1}{2}(h_1+h_3)\right) = \frac{EI_T}{g(1+\mathrm{i}\beta)}\left[w^{iv} + g(1+\mathrm{i}\beta)(1+Y)w'' + \Omega^2 w\right]. \tag{A.5}$$

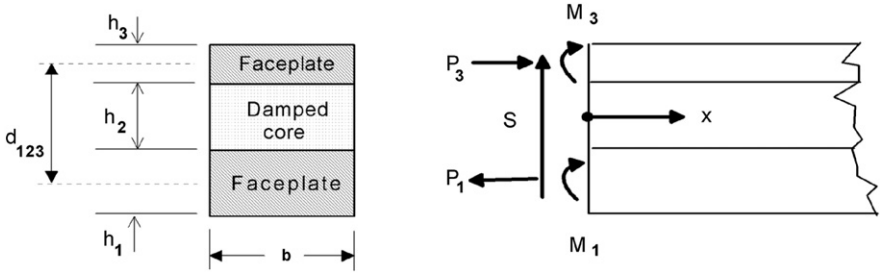

Fig. A.1. Dimensions and loads on the cross-section of a sandwich beam.

The boundary conditions at the ends $x = \pm L/2$ of the free–free beam are $S = 0$, $M = 0$ and $P = 0$ With $w(L/2)$ expressed in the form $w(L/2) = \sum_{n=1}^{3} A_{cn} \cosh(\lambda_n/2)$, these three equations become

$$S(L/2) = \sum_{n=1}^{3} A_{Cn} \sinh(\lambda_n/2)\left[\lambda_n^5 + g(1+\mathrm{i}\beta)(1+Y)\lambda_n^3 + \Omega^2\lambda_n\right] = \sum_{n=1}^{3} A_{Cn} F_S(\lambda_n, \Omega^2) = 0, \tag{A.6a}$$

$$P(L/2) = \sum_{n=1}^{3} A_{Cn} \cosh(\lambda_n/2)\left[\lambda_n^4 + g(1+\mathrm{i}\beta)\lambda_n^2 + \Omega^2\right] = \sum_{n=1}^{3} A_{Cn} F_P(\lambda_n, \Omega^2), \tag{A.6b}$$

$$M(L/2) = \sum_{n=1}^{3} A_{Cn} \cosh(\lambda_2/2)\left[\lambda_n^4 + g(1+\mathrm{i}\beta)(1+Y)\lambda^2 + \Omega^2\right] = \sum_{n=1}^{3} A_{Cn} F_M(\lambda_n, \Omega^2) = 0. \tag{A.6c}$$

The complex resonance frequency $\Omega^2(1+\mathrm{i}\eta)$ of a damped normal mode is found by making, in the first place, a reasonable guess at its real part and putting $\eta = 0$. Three corresponding λ's are then found from Eq. (10), followed by a process of iteration to find the accurate value of $\Omega^2(1+\mathrm{i}\eta)$, which satisfies the above three equations and are the Ω^2 roots of the determinantal equation

$$\begin{vmatrix} F_S(\lambda_1, \Omega^2), & F_S(\lambda_2, \Omega^2), & F_S(v_3, \Omega^2) \\ F_P(\lambda_1, \Omega^2), & F_P(\lambda_2, \Omega^2), & F_P(\lambda_3, \Omega^2) \\ F_M(\lambda_1, \Omega^2), & F_M(\lambda_2, \Omega^2), & F_M(\lambda_3, \Omega^2) \end{vmatrix} = |[F_{\mathrm{frfr}}]| = 0, \tag{A.7}$$

$[F_{\mathrm{frfr}}]$ signifying that this matrix pertains to the free–free beam.

Now consider the encastré beam, fully fixed at each of its ends. At $x = \pm L/2$ the two boundary conditions are simple, $w = 0, w' = 0$. These lead to two simple equations for the A_{Cn}'s:

$$w(L/2) = \sum_{n=1}^{3} A_{Cn} \cosh(\lambda_2/2) = \sum_{n=1}^{3} A_{Cn} F_w(\lambda_n, \Omega^2) = 0, \tag{A.8a}$$

$$w'(L/2) = \sum_{n=1}^{3} A_{Cn} \lambda_n \sinh(\lambda_n/2) = \sum_{n=1}^{3} A_{Cn} F_{w'}(\lambda_n, \Omega^2) = 0. \tag{A.8b}$$

The remaining boundary condition relates to the longitudinal displacements $u(x)$ in the face-plates which are zero at $x = L/2$. Hence, $u_1(L/2) = u_3(L/2) = 0$ and in terms of the three constituent waves they yield

$$u_1(L/2) = -\left[\frac{g(1+\mathrm{i}\beta)\,Y\,EI_T}{E_1 h_1 d_{123}}\right] \sum_{n=1}^{3} A_{Cn} \left\{\frac{\lambda_n L}{\lambda_n^2 - g(1+\mathrm{i}\beta)}\right\} \cosh(\lambda_n/2) = 0.$$

If this is satisfied, $u_3(L/2)$ is also zero.

The constant term preceding the summation can be dropped to give

$$u_1(L/2) = \sum_{n=1}^{3} A_{Cn} \left\{\frac{\lambda_n L}{\lambda_n^2 - g(1+\mathrm{i}\beta)}\right\} \cosh(\lambda_n/2) = \sum_{n=1}^{3} A_{Cn} F_n(\lambda_n, \Omega^2) = 0, \tag{A.8c}$$

Ω and η for the encastré beam are now found from the complex frequency roots of the determinantal equation

$$\begin{vmatrix} F_w(\lambda_1, \Omega^2), & F_w(\lambda_2, \Omega^2), & F_w(\lambda_3, \Omega^2) \\ F_{w'}(\lambda_1, \Omega^2), & F_{w'}(\lambda_2, \Omega^2), & F_{w'}(\lambda_3, \Omega^2) \\ F_u(\lambda_1, \Omega^2), & F_u(\lambda_2, \Omega^2), & F_u(\lambda_3, \Omega^2) \end{vmatrix} = |[F_{\mathrm{enc}}]| = 0, \tag{A.9}$$

$[F_{\mathrm{enc}}]$ signifying that the matrix pertains to the encastré beam.

The above equations and matrices are also involved in the equations for the response of the beams to a transverse point harmonic force. First of all, the wave field in an infinite beam due to a single force at the x-origin of the beam ($x = 0$) must be found. In the positive x-domain of the beam it consists of three damped

waves with wavenumbers having negative real parts, i.e.

$$w_+(x) = \sum_{n=1}^{3} A_{\infty,n} e^{-k_n x}, \tag{A.10}$$

the negative sign being included in the index simply to emphasise that these wavenumbers must have negative real parts.

There are three known boundary conditions at $x = 0$ which allow the A'_∞'s to be found in terms of the applied harmonic force $Fe^{i\omega t}$. They are $dw/(dx_{x=0}) = 0$, $S(0) = F/2$ and $u(0) = 0$. One obtains from these:

$$\sum_{n=1}^{3} A_{\infty,n}\lambda_n = 0, \tag{A.11a}$$

$$\sum_{n=1}^{3} A_{\infty,n}\left[\lambda_n^5 + g(1+i\beta)(1+Y)\lambda_n^3 + \Omega^2\lambda_n\right] = \sum_{n=1}^{3} A_{\infty,n}F_{\infty,s0}(\lambda_n,\Omega^2) = F/2 \tag{A.11b}$$

and

$$\sum_{n=1}^{3} A_{\infty,n}\left\{\frac{\lambda_n L}{\lambda_n^2 - g(1+i\beta)}\right\} = \sum_{n=1}^{3} A_{\infty,n}F_{\infty,u0}(\lambda n,\Omega^2) = 0, \tag{A.11c}$$

which have the matrix form

$$\begin{bmatrix} \lambda_1, & \lambda_2, & \lambda_3, \\ F_{\infty S0}(\lambda_1,\Omega^2), & F_{\infty S0}(\lambda_2,\Omega^2), & F_{\infty S0}(\lambda_3,\Omega^2) \\ F_{\infty u0}(\lambda_1,\Omega^2), & F_{\infty u0}(\lambda_2,\Omega^2), & F_{\infty u0}(\lambda_3,\Omega^2) \end{bmatrix} \begin{Bmatrix} A_{\infty,1} \\ A_{\infty,2} \\ A_{\infty,3} \end{Bmatrix} = [F_{\infty 0}]\{A_\omega\} = \begin{Bmatrix} 0 \\ 1 \\ 0 \end{Bmatrix} F/2. \tag{A.12}$$

Hence

$$\{A_\omega\} = [F_{\infty 0}]^{-1} \begin{Bmatrix} 0 \\ 1 \\ 0 \end{Bmatrix} F/2. \tag{A.13}$$

By analogy with Eq. (A.7), the shear force, face-plate axial force and bending moment due to this 'infinite' wave field at $x = L/2$ can be expressed in the form $[F_{\infty L/2}]\{A_\infty\}$. $[F_{\infty L/2}]$ has exactly the same form as $[F_{\text{frfr}}]$in Eq. (A.7) but its hyperbolic terms are all replaced by the appropriate exponential terms, $\exp \lambda_n/2$.

The reverberant wave field $\{A_{\text{REV}}\}$ caused by reflection of $\{A_\omega\}$ at the boundaries generates the forces and moment at $x = L/2$ given by $[F_{\text{frfr}}]\{A_{\text{REV}}\}$. ($[F_{\text{frfr}}]$ as defined in Eq. (A.7)). The total force and moment vector from the infinite and reverberant wave fields is therefore $[F_{\text{frfr}}]\{A_{\text{REV}}\} + [F_{\alpha L/2}]\{A_\omega\}$. It must vanish at the ends of the free–free beam, hence

$$\{A_{\text{REV}}\} = -[F_{\text{frfr}}]^{-1}[F_{\infty L/2}]\{A_\omega\} = -[F_{\text{frfr}}]^{-1}[F_{\infty L/2}][F_{\infty 0}]^{-1}[0,\ 1,\ 0]^{\text{T}}F/2. \tag{A.14}$$

An expression of identical form applies to the encastré beam, but with $[F_{\text{frfr}}]$ replaced by $[F_{\text{enc}}]$.

The total displacement $w(x)$ at any point in the beam is now given by

$$w(x) = \sum_{n=1}^{3}\left[A_{\infty,n}e^{-\lambda_n x/L} + A_{\text{REV},n}\cosh(\lambda_n x/L)\right]. \tag{A.15}$$

References

[1] H. Oberst, K. Frankenfeld, Über die Dämpfung der Biegeschwingungen dünner Bleche durch festhaftende Beläge: I Miteilung aus der Physikalisch-Technischen Bundesanstalt, *Acustica 2 Akustische Beihefte* 4 (1952) 181–194.

[2] D. Ross, E.E. Ungar, E.M. Kerwin Jr., Damping of plate flexural vibrations by means of visco-elastic laminae, structural damping, *American Society of Mechanical Engineers* (1959) 49–87.

[3] E.M. Kerwin Jr., Damping of flexural waves by a constrained viscoelastic layer, *Journal of the Acoustical Society of America* 31 (1959) 952–962.
[4] R.A. DiTaranto, Theory of the vibratory bending of a damped sandwich layer in non-sinusoidal modes, *Transactions of the American Society of Mechanical Engineers, Journal of Applied Mechanics* 87 (Ser. E) (1965) 881–886.
[5] D.J. Mead, S. Markus, The forced vibration of a three-layer, damped sandwich beam with arbitrary boundary conditions, *Journal of Sound and Vibration* 10 (1969) 163–175.
[6] D.J. Mead, S. Markus, Loss factors and resonant frequencies of encastré damped sandwich beams, *Journal of Sound and Vibration* 12 (1970) 99–112.
[7] E.E. Ungar, E.M. Kerwin Jr., Loss factors of viscoelastic systems in terms of energy concepts, *Journal of the Acoustical Society of America* 34 (1962) 954–957.
[8] D.J. Mead, The existence of normal modes of linear systems with arbitrary damping, in: *Symposium on Structural Dynamics*, Paper C9, Loughborough University, UK, 1970.
[9] Y.P. Lu, B.E. Douglas, On the forced vibrations of three-layer damped sandwich beams, *Journal of Sound and Vibration* 32 (1974) 513–516.
[10] D.J. Mead, *Passive Vibration Control*, Wiley, Chichester, UK, 1998.
[11] D.J. Mead, Y. Yaman, The harmonic response of rectangular sandwich plates with multiple stiffening: a flexural wave analysis, *Journal of Sound and Vibration* 145 (1991) 409–428.
[12] C.C. Kennedy, C.D.P. Pancu, Use of vectors in vibration measurement and analysis, *Journal of Aeronautical Sciences* 14 (1947) 603–605.